

## Microtexture and Strain in Electroplated Copper Interconnects

**R.Spolenak\*, D. L. Barr\*, M. E. Gross\*, K. Evans-Lutterodt\*, W. L. Brown\*, N. Tamura†, A. A. Macdowell†, R. S. Celestre†, H. A. Padmore†, B. C. Valek%, J. C. Bravman%, P. Flinn%, T. Marieb!, R. R. Keller\$, B. W. Batterman†§ and, J. R. Patel†§**

\* Bell Labs/Lucent Technologies, Murray Hill, NJ

† Advanced Light Source, Lawrence Berkeley National Lab., Berkeley, CA

% Dept. of Materials Science and Engineering, Stanford University, Stanford, CA

! Intel Corporation, Portland, OR

\$ National Institute of Standards and Technology, Materials Reliability Division, Boulder, CO

§ SSRL/SLAC, Stanford University, Stanford, CA

### ABSTRACT

The microstructure of narrow metal conductors in the electrical interconnections on IC chips has often been identified as of major importance in the reliability of these devices. The stresses and stress gradients that develop in the conductors as a result of thermal expansion differences in the materials and of electromigration at high current densities are believed to be strongly dependent on the details of the grain structure. The present work discusses new techniques based on microbeam x-ray diffraction (MBXRD) that have enabled measurement not only of the microstructure of totally encapsulated conductors but also of the local stresses in them on a micron and submicron scale. White x-rays from the Advanced Light Source were focused to a micron spot size by Kirkpatrick-Baez mirrors. The sample was stepped under the micro-beam and Laue images obtained at each sample location using a CCD area detector. Microstructure and local strain were deduced from these images. Cu lines with widths ranging from 0.8  $\mu\text{m}$  to 5  $\mu\text{m}$  and thickness of 1  $\mu\text{m}$  were investigated. Comparisons are made between the capabilities of MBXRD and the well established techniques of broad beam XRD, electron back scatter diffraction (EBSD) and focused ion beam imaging (FIB).

### INTRODUCTION

Currently, many companies are in the transition of dramatically changing their materials and processes for the multilevel interconnect structure in IC manufacturing. Well-known materials like aluminum and silicon dioxide are being replaced by copper and low-k dielectrics and the process architecture is changing from subtractive metal to damascene. The reliability of the new materials and structures has to be assessed and basic research and novel techniques are needed to gain the knowledge required for understanding their properties. For aluminum, stress gradients and high local stresses have been considered to be responsible for failure modes such as stress voiding and electromigration<sup>1,2</sup>. The measurement of stresses on a local (submicron) length scale has been found to be extremely difficult<sup>3-7</sup>. Even the non-destructive determination of the crystallographic orientation of buried single grains has recently only been accomplished by MBXRD<sup>3,6</sup>.

In this paper we will demonstrate how an x-ray microbeam can be used to determine the orientation and the strain in single Cu grains and to produce orientation and stress maps of entire line segments. This new technique will be compared to established techniques such as XRD, EBSD and FIB imaging.

### EXPERIMENTAL

The x-ray source for this experiment was the advanced light source (ALS) at the Lawrence Berkeley National lab (LBNL). An intense white x-ray beam (6 – 14 keV) was generated by a

bending magnet and focused to a spot size of  $0.8 \times 0.7 \text{ } \mu\text{m}^2$  by a pair of elliptically bent Kirkpatrick-Baez mirrors. Laue patterns were acquired using a CCD area detector positioned 30 mm above the sample, which was tilted at  $45^\circ$  relative to the x-ray beam. The indexing of the Laue patterns yields the crystallographic orientation of the grains. The deviation of the position of the Laue spots from the predicted position they would have for an unstrained cubic crystal, allows for the determination of the deviatoric component of the strain tensor. Typically 8 to 10 reflections from single grains were used to evaluate the deviation. In order to obtain the dilatational component of the strain tensor the exact energy of each reflection was determined by using a four-crystal Ge monochromator. The stress tensor is calculated from the complete strain tensor by using the tensor of the elastic constants. The geometry of the four-crystal monochromator allows for illuminating the sample at the same spot as with white light. The monochromator was calibrated to within 1 eV.

Custom-made software was used to determine the orientation, the deviatoric part of the strain tensor in every pixel and the energy of selected reflections. It was possible to index even multiple grains within the illuminated volume. Further details of the technique can be found in Tamura *et al.*<sup>8,9</sup>

The samples examined in this work were single level damascene Cu lines especially designed for *in situ* electromigration experiments. Single Cu line segments were connected electrically by Ta links. The line width ranged from  $0.8 \text{ } \mu\text{m}$  to  $5 \text{ } \mu\text{m}$  and the line thickness was  $1 \text{ } \mu\text{m}$ . The dielectric used was PE-TEOS and the samples were either uncapped or capped by 200 nm of  $\text{SiN}_x$ . The trenches etched in the dielectric were lined with a Ta barrier layer and a sputtered Cu seed layer and filled with electroplated Cu from an Enthone bath. All samples were annealed at  $400^\circ\text{C}$  for 30 min prior to the experiment.

## RESULTS

The first set of experiments studied uncapped Cu samples. Figure 1 shows maps of the orientation as well as of the deviatoric strain components in a  $5 \text{ } \mu\text{m}$  wide Cu line segment. The pixel size is  $0.5$  by  $0.5 \text{ } \mu\text{m}^2$ . The gray level of the orientation map corresponds to the angle between the (111) crystal orientation and the normal to the sample surface. Black area in general reflects the absence of data. The horizontal black line in the maps in Figure 1 and the black area in the lower right corner are two such regions. Two orientation maps are shown, which were produced by stepping the sample under the x-ray beam. When the x-ray illuminated volume in the sample consists of more than one grain, composite Laue patterns are obtained. The analysis software is able to index more than ten grains in such a case, as long as each grain is represented by at least six reflections. In the left MBXRD map in Figure 1 (“big grains”) only the grains with the strongest reflections within a pixel are shown. In the second map (“small grains”) the grains with the second strongest reflections are shown revealing a more detailed microstructure. When comparing the second map to the FIB image in the figure, areas of smaller grains, typically twins, can be identified.

As described above, the deviatoric part of the strain tensor can also be determined by the white beam Laue images. Here, the stress components out of plane and across the line are shown. As only the deviatoric part is shown, the component along the line can be omitted, as it has to add up with the other parts to make the trace of the tensor zero. The stresses are not constant throughout a single grain. The largest tensile and compressive deviatoric stresses are found in the regions close to the grain boundaries. This can be seen even better in the map of the Von Mises stresses (second from the right), which are a measure of the maximum shear stresses within the sample.

The furthest right strip in Figure 1 shows an FIB image visualizing the surface grain structure at a high resolution. The topography visible within a single grain is an artifact of the FIB imaging. The FIB image shows more detail, but the grain structure visible in the orientation maps and the FIB image are in quite good agreement. The comparison between the x-ray orientation map and the EBSD map is fairly good. The EBSD map was taken after FIB imaging and suffered from FIB produced ion damage and topography.

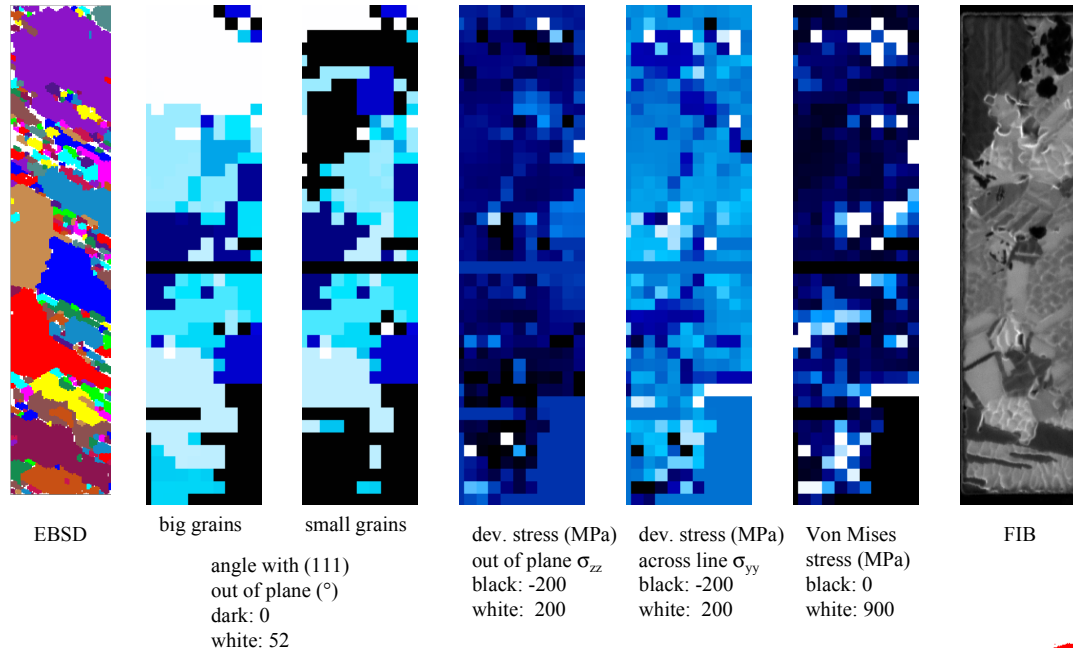


*Figure 1: orientation and stress maps for an uncapped damascene Cu line segment (5  $\mu\text{m}$  wide, 20  $\mu\text{m}$  long)*

Figure 2 shows results for a 2 micron wide uncapped damascene Cu line. The line is basically divided into a region with relatively big grains (in the lower half) and another with smaller grains. This can be seen in the orientation maps as well as the FIB image. In the “big grains” MBXRD map, which is based on only the strongest reflections in each pixel, the smaller grain with dark contrast in the FIB image (arrow) is not included. However, by discriminating against the most intense Laue reflections in each pixel, it shows up clearly in the “small grains” orientation map (second from the left). One has to bear in mind that MBXRD gives information about the entire volume of material, whereas an FIB image reveals only the structure closest to the surface.

In the deviatoric stress maps of Figure 2 only the strongest grains are shown. Here, the light (FIB) grain (see arrow) shows compressive deviatoric stresses (dark contrast) out of plane and tensile stresses across the line (light contrast).

Figure 3 shows results for a 2 micron wide line capped with 200 nm of  $\text{SiN}_x$ . This cap does not interfere with the MBXRD study of the line. The first map on the left shows again the angle between the (111) direction and the out of plane normal and thus also reveals the grain structure. In this case the grain structure is close to being bamboo. Here, the stresses measured not only originate from the post deposition thermal treatment, but also from an electromigration current of 0.5  $\text{MA}/\text{cm}^2$  that had been supplied for 20 hr at 300  $^\circ\text{C}$ . An interesting feature can be seen close to the grain boundary below a (111) oriented grain in the center of the segment. This can be seen in the compressive (dark) region in the deviatoric out of plane stress and in the tensile (white)

region in the stress across the line. The differences in the two deviatoric components leads to a significant Von Mises stress (white) in the same region.

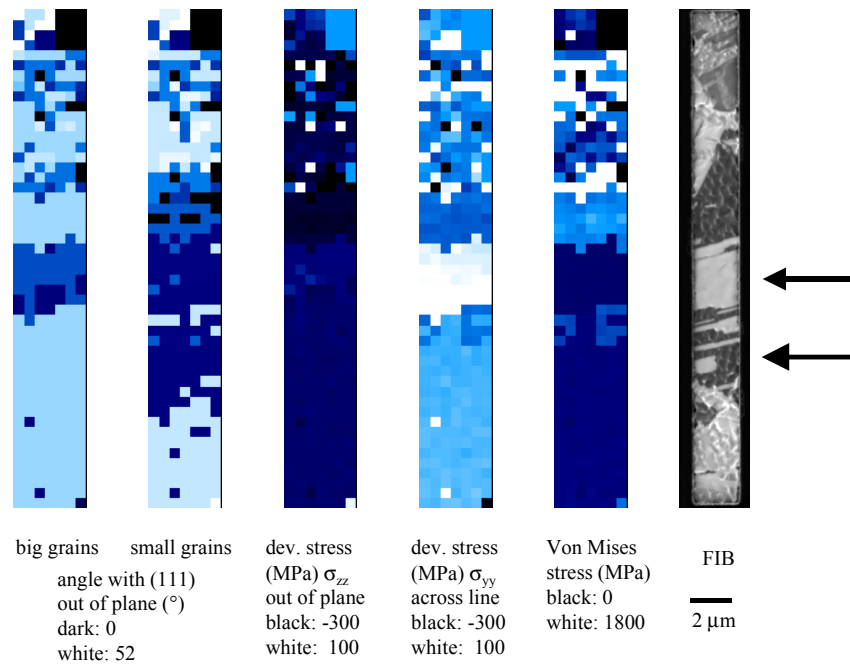


Figure 2: orientation and stress maps for an uncapped damascene Cu line segment (2  $\mu$ m wide, 20  $\mu$ m long)

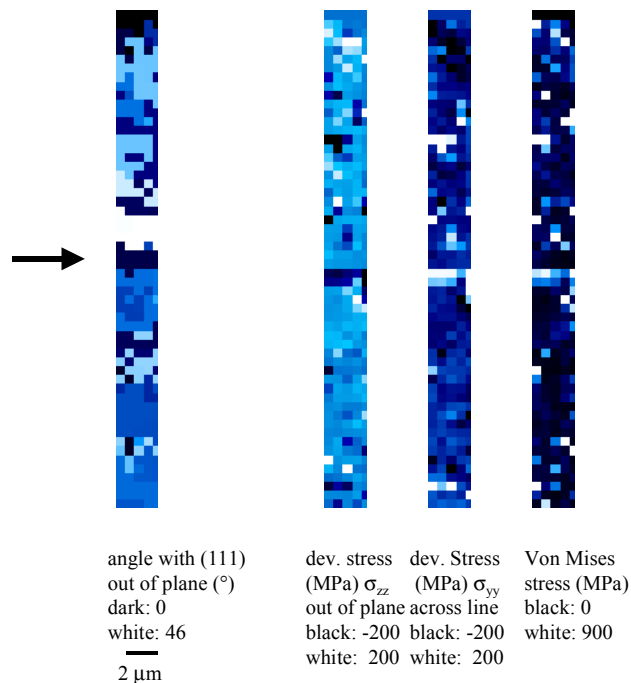


Figure 3: orientation and stress maps for a capped damascene Cu line segment (2  $\mu$ m wide, 30  $\mu$ m long)

Figure 4 shows the orientation components for a 0.8 micron wide line that is also essentially bamboo type. In addition to the overall orientation map three more narrowly defined maps are

shown emphasizing three different texture components. Three grains show a broad (111) texture, three to four seem to originate from a sidewall component or a second order twin and the majority belongs to a broad (115) texture. Results for the hydrostatic stress component for Al are shown in Tamura *et al.*<sup>8</sup>. The results for Cu will be shown in a future paper.

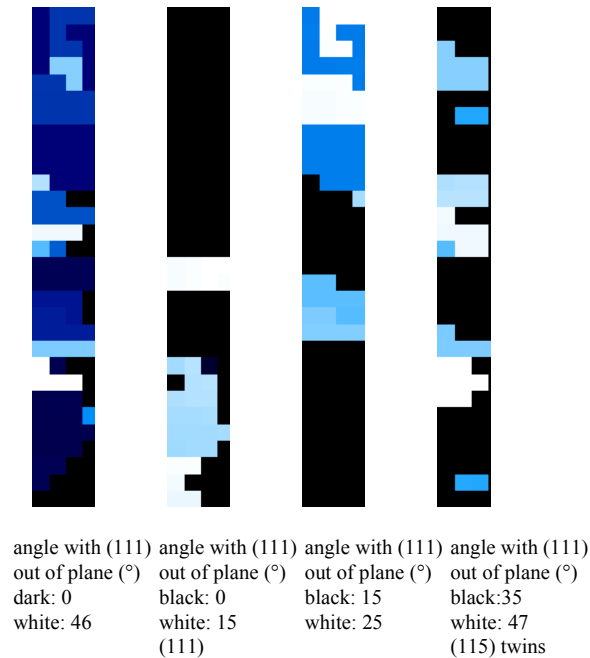


Figure 4: orientation maps for a capped damascene Cu line segment (0.8  $\mu\text{m}$  wide, 30  $\mu\text{m}$  long)

## DISCUSSION AND CONCLUSIONS

Considering the orientation maps of the different lines not many (111) oriented grains are observed. This observation is in contrast to the texture known from sputtered Cu films. However, it is agreement with observations made on annealed electroplated films<sup>10</sup>. The (115) twin texture had been found to be predominant. This is verified in the experimental results for the 0.8 micron wide line. Most of the grains are (115) oriented out of plane. Additionally, there is a (111) component and indications for a sidewall texture, a feature of electroplated Cu damascene that has been previously reported<sup>11</sup>. The manifold of texture components and the highly anisotropic elastic constants of Cu seem to be the origin of significant shear stresses, especially at grain boundaries as can be seen in Figures 1 to 3.

We have demonstrated the capabilities of a new method for orientation analysis and stress measurements on a submicron level. Table 1 shows the comparison between established techniques and this new x-ray technique. As in any local technique with a relatively long data acquisition time, the number of grains that can be analyzed is limited. For obtaining quantitative texture distributions conventional XRD is still the best approach. However, for the investigation of local phenomena, the local techniques are essential. At present FIB and EBSD have significantly better spatial resolution than the new MBXRD, however, they are limited to the analysis of volumes very close to the surface and cannot penetrate capping layers.

The strength of MBXRD is that it provides information from the entire volume of a thin film and that it in principle detects all grains that are present within the illuminated volume. The software mentioned above is able to identify more than ten grains within one Laue pattern. As

long as the exposure time is long enough to provide enough data for indexing at least six Laue spots all the grains within the illuminated volume can be identified. The second advantage compared to the other local techniques is the property of x-rays to penetrate capping layers. In this way materials properties can be studied without sample preparation that may change the stress state, which is a major drawback for CBED. By acquiring images at different detector distances even buried structures can be investigated and the origin of the reflections can be identified by triangulation. The most important feature of the MBXRD technique is its ability to provide the complete three-dimensional strain tensor for a single grain without changing the stress state through sample preparation. Provided the grain size is comparable to or bigger than the spot size, even strain variations within single grains can be detected.

	<b>XRD</b>	<b>FIB</b>	<b>EBSD</b>	<b>MBXRD</b>	<b>CBED</b>
<b>statistics</b>	good	medium	low	low	very low
<b>spatial resolution</b>	poor	5 nm	100 nm	800 nm	10 nm
<b>analyzed volume</b>	entire	surface	surface	entire	entire
<b>strain</b>	yes	no	no	yes	yes
<b>multiple grains</b>	yes	no	no	yes	no
<b>availability</b>	high	high	high	scarce	scarce
<b>measurement time</b>	fast/medium	fast	medium	slow	slow
<b>orientational</b>	1°	10°	1°	0.1°	0.5°
<b>accuracy</b>					
<b>sample preparation</b>	none	clean	clean	none	TEM prep.

*Table 1: Comparison of XRD (x-ray diffraction), FIB (focused ion beam), EBSD (electron back-scatter diffraction), MBXRD (microbeam x-ray diffraction) and CBED (convergent beam electron diffraction)*

Summarizing, this technique has the potential to become one of the key elements in the research of thin film phenomena on the micron and submicron scale. Reliability issues such as local plastic deformation caused by electromigration or thermal stresses are being investigated.

## ACKNOWLEDGEMENTS

The authors would like to thank the members of the SFRL (Silicon Fabrication Research Laboratory) namely, M. Buonanno, M. Hoover, S. Fiorillo, M. D. Morris, K. Takahashi, J. Frackowiak, T. Craddock, J. F. Miner, G. R. Weber, W. Mansfield, W. W. Tai, F. Klemens, A. Kornblit, R. Keller, and E. Ferry for their contributions in preparation of the samples.

## REFERENCES

1. I. A. Blech and K. L. Tai, Appl. Phys. Lett. **30** (8), 387-389 (1977).
2. P.-C. Wang, G. S. Cargill III, I. C. Noyan, and C.-K. Hu, Appl. Phys. Letters **72** (11), 1296-1298 (1998).
3. J.-S. Chung and G. E. Ice, J. Appl. Phys. **85**, 3546-3555 (1999).
4. S. Kraemer, J. Mayer, C. Witt, A. Weickenmeier, and M. Ruehle, Ultramicroscopy **81**, in press (2000).
5. H. J. Maier, R. R. Keller, H. Renner, H. Mughrabi, and A. Preston, Philosophical Magazine **A74**, 23-46 (1996).
6. N. Tamura, J.-S. Chung, G. E. Ice, B. C. Larson, J. D. Budai, and W. Lowe, Mat. Res. Soc. Symp. Proc. **563**, 175-180 (1999).
7. A. J. Wilkinson, Ultramicroscopy **62** (4), 237-247 (1996).
8. N. Tamura, B. C. Valek, R. Spolenak, A. A. MacDowell, R. S. Celestre, H. A. Padmore, W. L. Brown, J. C. Bravman, P. Flinn, T. Marieb, B. W. Batterman and, J. R. Patel, Mat. Soc. Rec. Proc. **submitted** (2000).

9. A. A. MacDowell, C. H. Chang, H. A. Padmore, J. R. Patel, and A. C. Thompson, Mat. Res. Soc. Proc. **524**, 55-58 (1998).
10. R. Spolenak, C. A. Volkert, K. M. Takahashi, S. A. Fiorillo, J. F. Miner, and W. L. Brown, Mat. Res. Soc. Proc. **in print** (1999).
11. C. Link, M. E. Gross, and W. L. Brown, Applied Physics Letters **74** (5), 682-684 (1999).